Published in final edited form as:
Free Radic Biol Med. 2011 July 1; 51(1): 160–170. doi:10.1016/j.freeradbiomed.2011.04.007.

Removal of H_2O_2 and generation of superoxide radical: Role of cytochrome c and NADH

Murugesan Velayutham[*], **Craig Hemann**, and **Jay L. Zweier**[*]
Center for Biomedical EPR Spectroscopy and Imaging, the Davis Heart and Lung Research Institute, and the Division of Cardiovascular Medicine, the Department of Internal Medicine, The Ohio State University College of Medicine, Columbus, Ohio 43210

Abstract

In cells, mitochondria, endoplasmic reticulum, and peroxisomes are the major sources of reactive oxygen species (ROS) under physiological and pathophysiological conditions. Cytochrome c (cyt c) is known to participate in mitochondrial electron transport and has antioxidant and peroxidase activities. Under oxidative or nitrative stress, the peroxidase activity of Fe^{3+}cyt c is increased. The level of NADH is also increased under pathophysiological conditions such as ischemia and diabetes and a concurrent increase in hydrogen peroxide (H_2O_2) production occurs. Studies were performed to understand the related mechanisms of radical generation and NADH oxidation by Fe^{3+}cyt c in the presence of H_2O_2. Electron paramagnetic resonance (EPR) spin trapping studies using 5,5-dimethyl-1-pyrroline-N-oxide (DMPO) were performed with NADH, Fe^{3+}cyt c, and H_2O_2 in the presence of methyl-β-cyclodextrin. An EPR spectrum corresponding to the superoxide radical adduct of DMPO encapsulated in methyl-β-cyclodextrin was obtained. This EPR signal was quenched by the addition of the superoxide scavenging enzyme Cu,Zn-superoxide dismutase (SOD1). The amount of superoxide radical adduct formed from the oxidation of NADH by the peroxidase activity of Fe^{3+}cyt c increased with NADH and H_2O_2 concentration. From these results, we propose a mechanism in which the peroxidase activity of Fe^{3+}cyt c oxidizes NADH to $NAD^{\bullet}$, which in turn donates an electron to O_2 resulting in superoxide radical formation. A UV-visible spectroscopic study shows that Fe^{3+}cyt c is reduced in the presence of both NADH and H_2O_2. Our results suggest that Fe^{3+}cyt c could have a novel role in the deleterious effects of ischemia/reperfusion and diabetes due to increased production of superoxide radical. In addition, Fe^{3+}cyt c may play a key role in the mitochondrial "ROS-induced ROS-release (RIRR)" signaling and in mitochondrial and cellular injury/death. The increased oxidation of NADH and generation of superoxide radical by this mechanism may have implications for the regulation of apoptotic cell death, endothelial dysfunction, and neurological diseases. We also propose an alternative electron transfer pathway, which may protect mitochondria and mitochondrial proteins from oxidative damage.

[*]Address correspondence to: Murugesan Velayutham, Ph.D, TMRF, Room 130, 420, W. 12th Avenue, The Ohio State University, Columbus, OH - 43210, Phone: 614-292-9082, Fax: 614-292-8454, Murugesan.Velayutham@osumc.edu, Jay L. Zweier, MD, Davis Heart and Lung Research Institute, 473 W. 12th Ave, Room 611C, The Ohio State University, Columbus, OH - 43210, Phone: 614-247-7788, Fax: 614-292-8778, Jay.Zweier@osumc.edu.

Keywords

EPR; superoxide radical; spin trapping; H_2O_2; ROS; DMPO; NADH; cytochrome c; peroxidase activity; ischemia; reperfusion; diabetes; ROS-induced ROS-release (RIRR); EPR oximetry

Introduction

In mammalian cells, mitochondria, endoplasmic reticulum, and peroxisomes are the major sources of reactive oxygen species (ROS) under physiological and pathophysiological conditions [1–3]. Under normal physiological conditions ~1–2% of the oxygen consumed by the heart is converted into reactive oxygen species (ROS) [4]. In heart, ~30 % of the total volume is occupied by mitochondria [5]. Electron leakage from the electron transport chain in mitochondria occurs with partial reduction of oxygen with generation of ROS [6]. In addition, sulfhydryl oxidases generate disulfide bonds with the reduction of oxygen to H_2O_2 in the mitochondrial intermembrane space (IMS) [7]. Cardiac ischemia leads to a decline in mitochondrial respiratory function that can be exacerbated upon reperfusion [8]. During ischemia (I) and reperfusion (R) in the heart, the production of reactive oxygen species (ROS) increases [8, 9]. ROS generation also increases under pathophysiological conditions such as diabetes, atherosclerosis, vascular and neurodegenerative diseases, and cancer [10]. The molecular mechanisms involved in the generation of ROS are not yet fully understood; therefore, it is necessary to unravel the source(s) and molecular mechanisms involved in the formation of ROS under pathophysiological conditions.

Under physiological conditions, NADH is a substrate for complex-I (NADH:ubiquinone oxidoreductase) in the electron transport chain (ETC) in mitochondria [11]. In the heart, the level of NADH increases during both ischemia and reperfusion as a consequence of anaerobic glycolysis [12–15]. Moreover, the level of NADH also increases under pathophysiological conditions such as diabetes and cancer [16, 17]. Recently, it was found that the increase in NADH oxidation induces a concurrent increase in superoxide radical production during ischemia [9]. Therefore, it is very crucial to explore the role of NADH in the generation of ROS during both ischemia and reperfusion in heart and under pathophysiological conditions such as diabetes.

Very recently, a study has shown that respiration-dependent detoxification of H_2O_2 protects rat brain mitochondria [18]. In addition, oxidized cyt c (Fe^{3+}cyt c) protects complex IV against H_2O_2 induced oxidative damage [19]. However, the role of mitochondrial proteins and molecular mechanisms involved in the removal of H_2O_2 are not fully understood.

Cytochrome c (cyt c) is a small, globular heme protein which exists in high concentration (0.5 – 5 mM) in the inner membrane of mitochondria [20]. At least 15 % of cyt c is tightly bound to the inner membrane and the remainder is loosely attached to the inner membrane and can be readily mobilized [21]. Physiologically, cyt c mediates electron shuttling between cytochrome c reductase (complex III) and cytochrome c oxidase (complex IV) during mitochondrial respiration [21]. The loosely associated cyt c participates in electron transport, mediates superoxide removal and prevents oxidative stress [21–23] while the tightly bound cyt c accounts for the peroxidase activity [24]. Upon interaction with cardiolipin, a mitochondria-specific phospholipid, cyt c has been shown to alter its tertiary structure and gain peroxidase activity [25]. Under conditions of oxidative and nitrosative stress, the peroxidase activity of cyt c also increases [26, 27]. Release of cyt c from the inner mitochondrial membrane into the cytosol is a proapoptotic factor [28, 29]. In the early event of apoptosis, the redox function of cyt c in the respiratory chain switches to a peroxidase function [25, 30]. The increased peroxidase activity of cyt c is implicated in various

neurodegenerative diseases, such as Parkinson's disease, Alzheimer's disease, and amyotrophic lateral sclerosis (ALS) [31]. In order to gain a better understanding of the role of Fe^{3+}cyt c in oxidative damage, pathological conditions, and removal of H_2O_2, we have employed the powerful, sensitive, and specific technique of electron paramagnetic resonance (EPR) spin trapping along with UV-visible absorption spectroscopy to investigate the oxidation of NADH and generation of free radicals by the peroxidase activity of Fe^{3+}cyt c and redox change of cyt c.

Materials and methods

Materials

Oxidized cytochrome c (Fe^{3+}cyt c, from horse heart), hydrogen peroxide (H_2O_2), NADH and sodium hypochlorite (4% chlorine available in solution) were purchased from Sigma. Diethylenetriaminepentaacetic acid (DTPA), 2,2,6,6-tetramethyl-1-piperidinyloxy (TEMPO), and methyl-β-cyclodextrin (Me-β-CD) were obtained from Aldrich. Purified 5,5-Dimethyl-1-pyrroline-*N*-oxide (DMPO) was purchased from Dojindo laboratories, Kumamoto, Japan. Microcrystalline particulate of lithium phthalocyanine (LiPc) was synthesized in our laboratory and used as an oximetry probe [32].

Preparation of the HOCl- oxidized Fe^{3+}cyt c (M-Fe^{3+}cyt c)

M-Fe^{3+}cyt c was prepared as describe previously [26]. Fe^{3+}cyt c (1 mM) was incubated with HOCl (4 mM) at room temperature for 15 minutes. The reaction mixture was diluted ten fold and concentrated with an Amicon Ultra-4 5000 MWCO concentrator. This process was repeated five times to remove excess HOCl.

EPR measurements

EPR spectra were recorded using quartz flat cells at room temperature with a Bruker ESP 300 or 300E spectrometer operating at X-band with 100 kHz modulation frequency and a TM_{110} cavity. Room temperature EPR spectra were recorded using the following parameters: microwave frequency 9.779 GHz, modulation frequency 100 kHz, modulation amplitude 1 G, microwave power 20 mW, number of scans 10, scan time 30 s, and time constant 82 ms. EPR spectral recording began two minutes after the addition of H_2O_2. All the experiments were carried out in phosphate buffer (50 mM and pH 7.4) containing 0.1 mM DTPA. Reactions were initiated by the addition of H_2O_2. Experiments were performed under anaerobic conditions by preparing the reaction mixture followed by transfer to quartz flat cell that was then sealed inside a nitrogen filled glove box.

Quantitation of the observed free radical signals was performed by computer simulation of the spectra with comparison of the double integral of the observed signal to that of a TEMPO standard (1 μM) measured under identical conditions [33].

EPR oximetry experiments were carried out as described previously [34].

UV-visible spectrophotometry

Optical spectra were measured on a Cary 50 Bio UV-visible spectrophotometer. The concentration of hypochlorite (HOCl) was measured by using the molar extinction coefficient of hypochlorite ($\varepsilon_{292\ nm}$ = 350 $M^{-1}cm^{-1}$) in 5 mM sodium hydroxide solution at pH 11–12 [35].

The reduction of Fe^{3+}cyt c was carried out in phosphate buffer (50 mM and pH 7.4) containing 0.1 mM DTPA. Reactions were initiated by the addition of H_2O_2. UV-visible spectra were recorded five minutes after the addition of H_2O_2.

Results

EPR spin trapping studies of the generation of superoxide radical by Fe^{3+}cyt c in the presence of NADH and H_2O_2

It has been demonstrated that Fe^{3+}cyt c acts as a peroxidase and is involved in the detoxification of H_2O_2 [24]. During peroxidase activity, Fe^{3+}cyt c reacts with H_2O_2 to form the peroxidase compound I-type intermediate, as shown in Scheme 1. The peroxidase activity of Fe^{3+}cyt c oxidizes various endogenous antioxidants such as ascorbate, GSH, and NADH in the presence of H_2O_2, as shown in Scheme 1 [36].

The levels of NADH in the ischemic and post-ischemic reperfused hearts are higher than in the normal heart [14]. The level of NADH decreases during post-ischemic reperfusion in the heart [14]. To gain insight into the molecular mechanisms involved in the formation of ROS during ischemia-reperfusion, we wanted to study the oxidation of NADH and free radical generation by the Fe^{3+}cyt c and H_2O_2 system. EPR spin trapping is a powerful technique to study ROS formation. EPR spin trapping studies using the spin trap DMPO were carried out to investigate the oxidation of NADH by Fe^{3+}cyt c and H_2O_2. EPR specta were recorded from Fe^{3+}cyt c (0.1 mM) in the presence of H_2O_2 (0.5 mM), NADH (1 mM), DMPO (50 mM), and Me-β-CD (0.1 M) along with DTPA (0.1 mM). A prominent EPR signal was seen corresponding to the superoxide radical adduct of DMPO (DMPO-OOH), as shown in Figure 1A. From the EPR spectrum the calculated isotropic hyperfine values are a_N = 13.49 G, a_{H1} = 10.78 G, and a_{H2} = 1.39 G, which are in agreement with reported values [37]. In the absence of Fe^{3+}cyt c, a trace level of DMPO-OOH signal was obtained, as shown in Figure 1B. A very weak quartet EPR signal of intensity ratio 1:2:2:1 was obtained in the absence of Me-β-CD, as shown in Figure 1C. From the EPR spectrum, the calculated isotropic hyperfine coupling constant is 14.9 G ($a_N = a_H$), which corresponds to the hydroxyl radical adduct of DMPO (DMPO-OH). To confirm that the superoxide radical is generated in the reaction mixture, addition of superoxide radical scavenging enzyme, Cu,Zn-superoxide dismutase (SOD1), to the reaction mixture quenched the EPR signal, as shown in Figure 1D. In the absence of NADH, an EPR signal indicative of the direct oxidation of DMPO to DMPO-X was obtained, as shown in Figure 1E. No EPR signal was obtained in the absence of H_2O_2, as shown in Figure 1F. These results show that superoxide radical is generated during the oxidation of NADH by the Fe^{3+}cyt c in the presence of H_2O_2.

The level of ROS and NADH are increased under various pathological conditions such as ischemia, ischemia-reperfusion, and diabetes [10, 14, 16]. EPR spin trapping studies were carried out with varying concentrations of NADH and H_2O_2. The NADH concentration dependence of superoxide radical formation is shown in Figure 2. The EPR signal intensity increases with increasing NADH concentration (Figure 2). The plot of concentration of DMPO-OOH vs time for various concentrations of NADH is shown in Figure 3A. A plot of the initial rate of formation of DMPO-OOH vs concentration of NADH is linear up to 1 mM and decreases at higher concentration of NADH (2 mM) (Figure 3B).

The H_2O_2 concentration dependence of superoxide radical formation is shown in Figure 4. The EPR signal intensity increases with increasing H_2O_2 concentration (Figure 4). The plot of concentration of DMPO-OOH vs time for various concentrations of H_2O_2 is shown in Figure 5A. A plot of the initial rate of formation of DMPO-OOH vs concentration of H_2O_2 is linear up to 0.5 mM as shown in Figure 5B. These results show that formation of superoxide radical increases with increasing levels of NADH and H_2O_2.

The oxygen dependence of superoxide radical formation during the oxidation of NADH by Fe^{3+}cyt c in the presence of H_2O_2 is shown in Figure 6. No EPR signal was observed in the absence of oxygen as shown in Figure 6A. In the presence of oxygen, an EPR spectrum

corresponding to the superoxide radical adducts of DMPO, DMPO-OOH, was obtained (see Figure 6B). This study shows that superoxide radical generation is oxygen dependent.

EPR oximetry studies of consumption of oxygen

The EPR spectrum of lithium phthalocyanine (LiPc) exhibits a single peak which is broadened by the presence of oxygen. The extent of broadening is a linear function of oxygen tension so that the change in broadening can be used to monitor oxygen consumption [34]. EPR oximetry experiments were performed for the reaction mixture containing Fe^{3+}cyt c (0.1 mM), NADH (1 mM), and H_2O_2 (0.5 mM) in phosphate buffer. A time-dependent sharpening of the line width was observed. The EPR line width is converted into partial pressure of oxygen using a standard calibration curve. From the known concentration of oxygen in aqueous solvent (water), 0.265 mM [38], the partial pressure of oxygen can also be converted into concentration units. Figure 7 shows a plot of this oxygen consumption data as a function of time.

EPR spin trapping studies of the generation of superoxide radical by HOCl-oxidized Fe^{3+}cyt c (M-Fe^{3+}cyt c) in the presence of NADH and H_2O_2

It has been shown that HOCl oxidizes methione-80 (M80) heme ligand in Fe^{3+}cyt c [26]. The oxidation of the M80 heme ligand resulted in the increased peroxidase activity of Fe^{3+}cyt c [26]. In order to understand the role of peroxidase activity of Fe^{3+}cyt c under pathophysiological conditions, we used EPR spin trapping experiments to study the oxidation of NADH and generation of superoxide radical by HOCl-oxidized Fe^{3+}cyt c (M-Fe^{3+}cyt c). The initial rates of formation of DMPO-OOH by Fe^{3+}cyt c and M-Fe^{3+}cyt c are shown in Figure 8. The initial rate of formation of DMPO-OOH by M-Fe^{3+}cyt is approximately three times higher than that of Fe^{3+}cyt c (see Figure 8). This study demonstrates that the increased peroxidase activity of M-Fe^{3+}cyt c increases the oxidation of NADH and generation of superoxide radical.

UV-visible absorption studies of reduction of Fe^{3+}cyt c in the presence of NADH and H_2O_2

The above EPR spin trapping studies have shown that superoxide radical is generated during the oxidation of NADH by Fe^{3+}cyt c in the presence of H_2O_2. It has been suggested that mitochondrial Fe^{3+}cyt c can oxidize superoxide radical under conditions of oxidative stress [22]. Both the superoxide radical and $NAD^{\bullet}$ reduce Fe^{3+}cyt c to Fe^{2+}cyt c (reduced cytochrome c) [22, 39, 40]. UV-visible spectrophotometry was used to explore the effect of oxidation of NADH by the peroxidase activity of Fe^{3+}cyt c on the redox change of Fe^{3+}cyt c, as shown in Figure 9. The UV-visible absorbance spectrum of phosphate buffer solution of Fe^{3+}cyt c (0.1 mM) in the wavelength range of 450–650 nm is shown in Figure 9A. No change in absorption spectrum was observed by the addition of H_2O_2 (0.5 mM) to the solution containing Fe^{3+}cyt c (0.1 mM), as shown in Figure 9B. A weak absorption at 550 nm was observed when NADH (2 mM) was added to the solution containing Fe^{3+}cyt c (0.1 mM), as shown Figure 9C. The absorption at 550 nm was further increased for the reaction mixture containing Fe^{3+}cyt c (0.1 mM), NADH (2 mM), and H_2O_2 (0.5 mM), as shown in Figure 9D. This study shows that oxidation of NADH by the peroxidase activity of Fe^{3+}cyt c reduces Fe^{3+}cyt c to Fe^{2+}cyt c.

The level of ROS and NADH are increased under various pathological conditions such as ischemia, ischemia-reperfusion, and diabetes [10, 14, 16]. UV-visible absorption spectroscopic studies were performed with varying concentrations of NADH and H_2O_2. The absorption at 550 nm, corresponding to Fe^{2+}cyt c, was followed with various concentrations of NADH as shown in Figure 10A. The absorption at 550 nm increases with increasing NADH concentration and it is linear up to 2 mM, as shown in Figure 10A.

The H_2O_2 concentration dependence of reduction of Fe^{3+}cyt c is shown in Figure 10B. The absorption at 550 nm was followed with various concentrations of H_2O_2. The absorption at 550 nm increases with increasing H_2O_2 concentration and it is linear up to 0.5 mM, as shown in Figure 10B. These studies show that reduction of Fe^{3+}cyt c increases with increasing levels of NADH and H_2O_2.

Discussion

In this study, the EPR spin trapping experiments were carried out in the presence of Me-β-CD to increase the half-life of the DMPO-OOH adduct. The EPR spectrum obtained for the reaction mixture in the absence of Me-β-CD corresponds to the hydroxyl radical adduct of DMPO, DMPO-OH (Figure 1C). The superoxide radical adduct of DMPO, DMPO-OOH, decomposes to DMPO-OH in aqueous solution with a half-life of approximately 45 s [37]. It has been shown that the half-life of DMPO-OOH was increased to 358 s by the addition of Me-β-CD, which forms an inclusion complex with DMPO-OOH [37]. The EPR spectrum corresponding to the superoxide radical adduct of DMPO, DMPO-OOH, was obtained for the reaction mixture containing DMPO, Me-β-CD, Fe^{3+}cyt c, NADH, and H_2O_2 (Figure 1A). Inclusion of the superoxide scavenging enzyme, SOD1, in the reaction mixture abolishes the EPR signal as shown in Figure 1D. This result shows that superoxide radical is generated in the reaction mixture containing Fe^{3+}cyt c, NADH, and H_2O_2.

In the absence of Fe^{3+}cyt c in the reaction mixture, a trace level of the DMPO-OOH signal was obtained. This EPR signal was due to the direct reaction between NADH and H_2O_2 (Figure 1B). This result suggests that the presence of Fe^{3+}cyt c in the reaction mixture catalyzes the oxidation of NADH in the presence of H_2O_2. In the absence of NADH in the reaction solution, a weak intensity EPR signal with the features corresponding to DMPOX was obtained (Figure 1E), which is due to the direct oxidation of DMPO by the peroxidase activity of cyt c (see scheme 1) [36]. No EPR signal was obtained in the absence of H_2O_2 in the reaction solution (Figure 1F). These results suggest that superoxide radical is generated in the presence of Fe^{3+}cyt c, NADH, and H_2O_2.

The EPR spectra in Figure 2 show that the intensity of the signal increases with an increasing concentration of NADH. The formation of DMPO-OOH increases with time for various concentrations of NADH, as shown in Figure 3A. These EPR spin trapping studies show that the peroxidase activity of Fe^{3+}cyt c oxidizes NADH and generates superoxide radical. The oxidation of NADH by the peroxidase activity of Fe^{3+}cyt c produces $NAD^{\bullet}$ [36], which in turn reacts with molecular oxygen to form NAD^+ and superoxide radical, as shown in Scheme 2 [41]. The second-order rate constant for the reaction of $NAD^{\bullet}$ with O_2 is $1.9 \times 10^9\ M^{-1}s^{-1}$ [41].

A plot of the initial rate of formation of DMPO-OOH as a function of NADH concentration is linear up to 1 mM (Figure 3B), indicating the first-order dependence on NADH concentration. However, at higher concentrations of NADH, the initial rate of formation of DMPO-OOH decreases. It has been shown that superoxide radical reacts with DMPO-OOH adducts and decreases its concentration [42]. Therefore, at higher concentrations of NADH the superoxide radical reacts with DMPO-OOH adducts decreasing the initial rate of formation of DMPO-OOH.

The EPR spectra in Figure 4 show that the intensity of the signal increases with an increasing concentration of H_2O_2. The formation of DMPO-OOH increases with time for various concentrations of H_2O_2 as shown in Figure 5A. A plot of the initial rate of formation of DMPO-OOH as a function of H_2O_2 concentration is linear (Figure 5B), indicating the first-order dependence on H_2O_2 concentration. These EPR spin trapping studies show that

the increased production of ROS (H_2O_2) increases the formation of the compound-I intermediate of Fe^{3+}cyt c, which oxidizes NADH to $NAD^{\bullet}$. These results show that the increased production of ROS (H_2O_2) induces increased production of superoxide radicals.

Cyt c is found in high concentrations (0.5– 5 mM) in the inner membrane of mitochondria [20]. It has been suggested that membrane bound cyt c may function as a competitive peroxidase [43]. Cardiolipin (CL) is an acidic phospholipid found primarily in the inner mitochondrial membrane and confers fluidity and stability to the membrane [44, 45]. Several components of the respiratory chain are critically dependent on their interaction with cardiolipin for optimal function. [44]. Cyt c is anchored to the mitochondrial membrane through both electrostatic and hydrophobic interactions with cardiolipin [44, 45]. The interaction of cardiolipin with cyt c forms a CL-cyt c complex, which breaks the Met80-Fe^{3+} bond and increases the accessibility of H_2O_2 to the active site of Fe^{3+}cyt c [46]. As a result of this, the peroxidase activity of CL-cyt c complex is increased more than 50-fold [43]. It has been estimated that the second order rate constant for the peroxidase activity of CL-cyt c complex is 200 $M^{-1}s^{-1}$ [47]. Hence, the lipophilic environment in the mitochondria enhances the peroxidase activity of Fe^{3+}cyt c

In normal tissues, the cellular levels of NADH have been measured in the range of 0.33 to 0.83 mM [48–50]. The level of NADH increases under starvation and pathophysiological conditions such as ischemia (reaches 1.85 mM), ischemia-reperfusion, and diabetes [14, 16, 50]. The intracellular concentration of H_2O_2 is approximately 1 μM [51, 52]. In rat brain tissue, the measured concentration of H_2O_2 is in the range of 2 – 4 μM [53]. Importantly, the level of ROS increases under various pathophysiological conditions, such as ischemia, ischemia-reperfusion, and diabetes [8, 10, 54]. Recently, it has been shown that the generation of H_2O_2 by the epithelial cells at wound margin in zebrafish larvae reaches 50 μM levels [55]. With a second order rate constant of 200 $M^{-1}s^{-1}$, the peroxidase activity of CL-cyt c can be readily detectable at H_2O_2 levels as low as 5−10 μM [47]. Therefore, the potential exists for the oxidation of NADH by the peroxidase activity of Fe^{3+}cyt c and generation of superoxide radical under certain *in vivo* pathophysiological conditions.

NADH is a substrate of complex I in the electron transport chain in the mitochondria [11]. It has been shown that the level of NADH increases during ischemia and reperfusion in isolated rabbit heart [12]. It has also been demonstrated that the mitochondrial NADH-oxidase activity increases during ischemia in rat and dog hearts [9, 56, 57]. The production of superoxide radical increases with the duration of ischemia and increased oxidation of NADH [9]. It has been proposed that the activity of the enzyme NADH-oxidase could play an important role in the damage caused by ROS in cardiac cells during ischemic conditions [9, 56, 57]. It has also been suggested that brief ischemia promotes superoxide radical generation specifically within complex III–IV in the electron transport chain in the mitochondria [9]. In addition, complex IV was activated during ischemia and suggested to play a role in the production of superoxide radical [9]. However, the site of superoxide radical production was not likely within complex IV [9]. Hence, questions remain regarding the enzyme and molecular mechanism responsible for the production of superoxide radical. In the electron transport chain, complex IV oxidizes Fe^{2+}cyt c, a crucial step in activating its peroxidase activity [21, 36]. Activated complex IV maintains an increased level of Fe^{3+}cyt c and this could enhance Fe^{3+}cyt c catalyzed superoxide radical production. Our EPR spin trapping study delineates a mechanism whereby stimulation of the NADH-oxidase activity of Fe^{3+}cyt c in the presence of H_2O_2 enhances superoxide radical production. Various studies have also reported that the production of superoxide radical deregulates mitochondria and causes apoptotic and necrotic cell death [4, 8]. These processes can ultimately result in heart failure [4, 8]. Our EPR spin trapping study implies that NADH and

Fe^{3+}cyt c may play an important role in oxidative damage during and following cardiac ischemia.

The level of ROS and oxygen varies among different tissues and under various pathological conditions such as post-ischemic reperfusion [8, 58, 59]. The level of oxygen and ROS increases during post-ischemic reperfusion [59]. Our EPR spin trapping results in Figure 6 show that no signal was observed in the absence of oxygen (Figure 6A). However, the introduction of oxygen in to the reaction mixture generates superoxide radical (Figure 6B). This study shows that the oxidation of NADH by the Fe^{3+}cyt c and H_2O_2 system in the presence of oxygen generates superoxide radical. Our EPR oximetry study, Figure 7, shows that oxygen is consumed during the oxidation of NADH by Fe^{3+}cyt c in the presence of H_2O_2. The initial rate of oxygen consumption observed was 1.53 μM/min. In corresponding UV-visible spectroscopic study, the initial rate of formation of superoxide radical was 1.19 μM/min. Our UV-visible results suggest that most of the oxygen consumed is reduced to form the superoxide radical.

A number of molecular mechanisms have been proposed to explain superoxide radical generation in the post-ischemic reperfused myocardium [8, 33]. The levels of NADH in the ischemic and post-ischemic reperfused hearts were higher than in the normal heart [12]. During post-ischemic reperfusion of the isolated heart, the levels of superoxide radical generation and NADH were increased and decreased respectively [8, 12, 14, 33]. In addition, the level of NAD^+ was increased during post-ischemic reperfusion [12]. From this observation, NADH was oxidized to NAD^+ during reperfusion. Moreover, the level of oxygen increases during post-ischemic reperfusion [59]. Therefore, it is essential to understand the molecular mechanism involved in the oxidation of NADH and production of superoxide radical during post-ischemic reperfusion. From our EPR spin trapping results, in the presence of H_2O_2 and oxygen, the NADH-oxidase activity of Fe^{3+}cyt c could be involved in the generation of superoxide radical during post-ischemic reperfusion.

It has been reported that in isolated rat hearts that the production of nitric oxide and superoxide radical are increased during the early period of post-ischemic reperfusion [60]. The increased production of nitric oxide reacted with superoxide radical to produce highly reactive peroxynitrite [60]. It is known that peroxynitrite and HOCl reacts with Fe^{3+}cyt c and modifies the co-ordination of iron in the heme through methionine 80 (M80-Fe) [26, 27, 61]. The coordination of heme iron in Fe^{3+}cyt c is also modified by nitrative and oxidative stresses [26, 27, 61, 62]. Further, the modified Fe^{3+}cyt c has increased peroxidase activity [26, 27, 61]. Our EPR spin trapping results show that oxidation of Fe^{3+}cyt c to M-Fe^{3+}cyt c by HOCl increases the oxidation of NADH and generation of superoxide radical (Figure 8). Hence, during postischemic reperfusion the increased peroxidase activity of Fe^{3+}cyt c could increase the production of superoxide radical by using NADH as a substrate.

In vitro, isolated rat heart mitochondria oxidize exogenous NADH [63]. Further, the oxidation of exogenous NADH by the liver mitochondria was increased in the presence of exogenously added Fe^{3+}cyt c [64, 65]. The Fe^{3+}cyt c catalyzed the oxidation of exogenous NADH and transferred the electron to molecular oxygen [65]. Our EPR spin trapping results show that Fe^{3+}cyt c in the presence of H_2O_2 catalyses the oxidation of NADH and produces superoxide radical. Under physiological and pathophysiological conditions, mitochondria produce H_2O_2 due to partial reduction of molecular oxygen [2]. The H_2O_2 produced by mitochondria could be used by the Fe^{3+}cyt c to oxidize NADH, producing superoxide radical. Further, the increased oxidation of NADH by the Fe^{3+}cyt c alters the mitochondrial permeability transition (MPT) [65]. It was also shown that in isolated rat liver mitochondria MPT pore opening induces ROS production in the presence of NADH [66]. In addition, MPT pore opening inhibits the ETC complex I activity and releases cytochrome c [66].

However, the mitochondrial enzyme involved in the oxidation of NADH and increased production of ROS is not clearly understood. Our study shows that Fe^{3+}cyt c catalyzes the oxidation of NADH and production of ROS in the presence of H_2O_2. It has been suggested that the Fe^{3+}cyt c and altered MPT play a role in cellular apoptosis and death [65, 67].

Several studies have also shown that in cardiac myocytes a distinct molecular mechanism is involved in increased ROS generation during excessive oxidative stress conditions such as ischemia/reperfusion [68–70]. In this mechanism, mitochondria can significantly amplify a low level of ROS in or around mitochondria as a cellular signal amplifier which is converted into a pathological ROS signal [68, 71]. It has been shown that the mitochondrial transition pore opening and ETC uncoupling are the main sources of increased generation of ROS during oxidative stress [68]. The increased generation of ROS in mitochondria results in "ROS-induced ROS-release" (RIRR) signaling [70,71]. The increased generation of ROS by the mitochondrial RIRR signaling results in mitochondrial and cellular injury/death and fatal arrhythmias [68, 69]. However, the molecular mechanisms involved in the increased generation of ROS by the mitochondrial RIRR signaling are not fully understood. Our EPR study shows that, in the presence of H_2O_2 (ROS), the oxidation of NADH by the Fe^{3+}cyt c results in the generation of superoxide radical (ROS). Hence, this RIRR activity of Fe^{3+}cyt c can play a major role in the mitochondrial RIRR signaling and in mitochondrial and cellular injury/death.

In heart, apoptosis increases during ischemia and reperfusion [72, 73]. Mitochondria are now recognized to play a critical role in mediating both apoptotic and necrotic cell death. The release of cyt c is an early step in apoptosis [28, 29]. In addition, the peroxidase activity of cyt c increases during apoptosis [61, 74]. Moreover, cardiolipin in mitochondria undergoes early oxidation during apoptosis [47]. The oxidation of cardiolipin is catalyzed by the CL-cyt c complex [47]. However, the oxidizing species responsible for the oxidation of cardiolipin is not fully understood. Apoptosis is associated with a massive depletion of NADH, as well as an increase in the generation of superoxide radical from the mitochondria [75, 76]. The increased generation of superoxide radical by the oxidation of NADH by the peroxidase activity of Fe^{3+}cyt c can play a major role in apoptosis. H_2O_2 is not a radical and less reactive. The oxidation of biological molecules by H_2O_2 is much weaker than superoxide radical [77]. Our EPR spin trapping results suggest that the superoxide radical may be involved in the oxidation of cardiolipin. Subsequently, the oxidized cardiolipin facilitates the release of cyt c from mitochondria during apoptosis. Various studies also have shown that during apoptosis superoxide radicals are generated along with cyt c release from the mitochondria [78, 79]. Recent studies have shown that cyt c was translocated to the cytoplasm and the nucleus in both apoptotic and nonapoptotic cells [61]. In nonapoptotic cells, the disruption of M80-Fe ligation stimulated the translocation of cyt c to the cytoplasm and nucleus [61]. The oxidation of the M80 heme ligand resulted in the increased peroxidase activity of Fe^{3+}cyt c [26, 80]. The present study shows that increased oxidation of NADH and generation of superoxide radical by the peroxidase activity of Fe^{3+}cyt c may have implications for the regulation of apoptotic cell death and translocation of cyt c to the cytoplasm and nucleus.

Diabetes affects various tissues and organs including micro- and macro-vasculature, heart, retina, liver, kidney and peripheral nerves [81]. Hyperglycemia in diabetes results in a shift of metabolism to the polyol/sorbitol pathway where there is an increased cytosolic NADH/NAD^+ ratio and level of ROS [16, 81]. Mitochondrial function has different implications for diabetes in different cells and tissues [81, 82]. The increased production of NADH and ROS are important in the pathogenesis of diabetes and its complications [16, 81]. It has been shown that mitochondrial functions, ROS production, and its components are critically involved in the pathophysiology of diabetes [81]. The superoxide radical production by the

oxidation of NADH by the peroxidase activity of Fe^{3+}cyt c suggests that this molecular mechanism may play a role in the pathophysiology of diabetes.

Biochemical studies have demonstrated NADH-oxidase as a major source of superoxide radical in vascular endothelium [83, 84]. In endothelial cells, the mitochondria play a major role in the production of ROS [82]. In endothelium, the increased production of superoxide radical results in the decreased availability of nitric oxide, which results in endothelial dysfunction [85]. Endothelial dysfunction is a hallmark of diseases comprehensively called endothelium-impaired function disorders, e.g. atherosclerosis, diabetes, hypertension, and heart failure [86]. It is well established that in rat vascular endothelium the production of superoxide radical anion is increased due to the increased oxidation of NADH [83, 84]. In a porcine model, H_2O_2 treatment increases the superoxide radical production in aortic vessels and endothelial cells [87]. In rat insulin-resistant aortas, NADH-oxidase derived superoxide radical impairs endothelium dependent vascular relaxation [88]. Still, the enzyme(s) responsible for the generation of superoxide radical anion using NADH as a substrate are not fully understood. From our EPR spin trapping study, it is possible that the NADH-oxidase activity of Fe^{3+}cyt c in the presence of H_2O_2 could be one of the pathways involved in the generation of superoxide radical anion in endothelial cells.

In a recent study, injection of Fe^{3+}cyt c along with H_2O_2 led to an increase in cell death in neuronal cells [89]. The increased peroxidase activity of Fe^{3+}cyt c is implicated in various neurodegenerative diseases, such as Parkinson's disease, Alzheimer's disease, and amyotrophic lateral sclerosis (ALS) [31]. Based on our EPR spin trapping results, we propose that the increased production of superoxide radical due to the oxidation of NADH by the Fe^{3+}cyt c and H_2O_2 system may be responsible for this increased neuronal cell death.

It has been suggested that mitochondrial Fe^{3+}cyt c can oxidize superoxide radical under conditions of oxidative stress [22]. Both the superoxide radical and $NAD^{\bullet}$ reduce Fe^{3+}cyt c into Fe^{2+}cyt c [22, 39, 40]. The absorption band at 550 nm is characteristic of the Fe^{2+}cyt c, which reflects the redox change of cyt c [40]. Our UV-visible spectroscopic study shows that there was a formation of an absorption band at 550 nm for the reaction mixture containing Fe^{3+}cyt c, NADH, and H_2O_2 (Figure 9D). In the absence of H_2O_2 in the reaction mixture, a weak absorption band at 550 nm was obtained (Figure 9C). This absorption band was due to the auto-oxidation of NADH. In the absence of NADH in the reaction solution, no change in the UV-visible absorption spectrum of Fe^{3+}cyt c was observed (Figure 9B). These results demonstrate that the reduction of Fe^{3+}cyt c is increased in the presence of both NADH and H_2O_2.

Under physiological conditions, in mitochondria, complex I and complex III produce ROS [2]. In addition, sulfhydryl oxidases generate disulfide bonds with the reduction of oxygen to H_2O_2 in the mitochondrial intermembrane space (IMS) [7]. H_2O_2, at intracellular concentrations less than 1 μM, is involved in regulatory processes [52, 90]. Intracellular H_2O_2 at concentrations above 1 μM is toxic to cells [52, 91]. In IMS there are no peroxidase enzymes, such as catalase, to remove the H_2O_2 [92]. In the respiratory chain, cyt c is necessary to keep the ROS at lower physiological levels [93]. It has been suggested that, under usual circumstances, the peroxidase activity of Fe^{3+}cyt c is an antioxidant, protective enzyme helping to remove excess H_2O_2 [47]. Various experimental results have shown that endogenous and exogenously added Fe^{3+}cyt c mediate the removal of H_2O_2 and protect mitochondria from oxidative damage [93–96]. It has been suggested that the peroxidase activity of CL-cyt c may favorably compete with other mitochondrial and peroxisomal H_2O_2 scavenging enzymes to control H_2O_2 levels at the expense of intracellular reductants [47]. Interestingly, Fe^{3+}cyt c, at higher concentrations, also protects cardiolipin and mitochondrial enzymes such as complex IV against H_2O_2-induced oxidative damage [19]. In this report, it

has been proposed that peroxidase activity is involved in the removal of H_2O_2 and suggested that electron donors are necessary for the removal of H_2O_2 [19]. Very recently, it has been shown that respiration-dependent detoxification of H_2O_2 protects rat brain mitochondria [18]. Therefore, certain molecular reactions are necessary to protect the mitochondria from oxidative damage as a result of production of H_2O_2. However, the molecular mechanisms involved in the removal of H_2O_2 by mitochondria are not fully understood. Our EPR spin trapping study shows that Fe^{3+}cyt c removes H_2O_2 using NADH as an electron donor and generates superoxide radical. A study on yeast has shown that cyt c is the most abundant protein in the mitochondrial intermembrane space [97]. Fe^{3+}cyt c acts as an antioxidant and converts superoxide radical into molecular oxygen [22]. It has also been shown that the superoxide radical and Fe^{3+}cyt c system can function as an electron donor for complex IV [22]. The $NAD^{\bullet}$ radical, formed during the oxidation of NADH by Fe^{3+}cyt c in the presence of H_2O_2, also reduces Fe^{3+}cyt c into Fe^{2+}cyt c [39]. Our UV-visible spectroscopic study shows that reduction of Fe^{3+}cyt c increases with increasing concentration of NADH and H_2O_2 (Figure 10).

In ETC, Fe^{2+}cyt c donates an electron to complex IV, which reduces molecular oxygen to water [2]. From our UV-visible spectroscopic study, Fe^{3+}cyt c in the presence of NADH removes H_2O_2 and facilitates the electron flow in ETC by scavenging superoxide radical and $NAD^{\bullet}$ and donates electrons to complex IV. In addition, Fe^{3+}cyt c protects complex IV from oxidative damage and supports complex IV to reduce molecular oxygen to water. Further, these molecular reactions involved in the alternative electron transfer pathway can protect the mitochondria from ROS induced oxidative damage. Our EPR and UV-visible spectroscopic studies show that Fe^{3+}cyt c in the presence of NADH may potentially play a role in the removal of H_2O_2 by the mitochondria. Based on our studies and reported literature, we propose that Fe^{3+}cyt c in the presence of NADH is involved in the removal of H_2O_2, generation of superoxide radical, and facilitation of electron flow in ETC as depicted in Figure 11.

In conclusion, the EPR results reported here show that Fe^{3+}cyt c in the presence of H_2O_2 oxidizes NADH and generates superoxide radical. Under conditions of oxidative stress, the increased peroxidase activity of Fe^{3+}cyt c increases the generation of superoxide radical. In addition to complex I–III, cyt c can also be another site of mitochondrial superoxide radical production. This work suggests that cyt c could have a novel role in the deleterious effects of ischemia/reperfusion and diabetes. The peroxidase activity of Fe^{3+}cyt c has important consequences on mitochondrial and cellular function and viability. Fe^{3+}cyt c may play a key role in the mitochondrial “ROS-induced ROS-release (RIRR)” signaling and in mitochondrial and cellular injury/death. Under certain conditions, Fe^{3+}cyt c mediated production of superoxide radical may also be involved in cell signaling pathways. The UV-visible spectroscopic results reported here demonstrate that Fe^{3+}cyt c in the presence of both H_2O_2 and NADH is reduced to Fe^{2+}cyt c. Hence, Fe^{3+}cyt c in the presence of NADH also plays a major role in the removal of H_2O_2 through an alternative electron transfer pathway and protects the mitochondria and mitochondrial proteins from ROS induced oxidative damage. These studies show that Fe^{3+}cyt c can have dual pro- and anti-oxidant properties and thus either a deleterious or protective role depending on the levels of NADH, H_2O_2, and Fe^{3+}cyt c. However, the biological relevance of these findings under various physiological and pathophysiological conditions such as oxidative damage during ischemia and reperfusion, diabetes, endothelial dysfunction, and neurological diseases remains to be elucidated.

Acknowledgments

This work was supported by National Institutes of Health Grants HL63744, HL65608, and HL38324 (JLZ).

References

1. Tu BP, Weissman JS. Oxidative protein folding in eukaryotes: mechanisms and consequences. J. Cell Biol. 2004; 164:341–346. [PubMed: 14757749]
2. St-Pierre J, Buckingham JA, Roebuck SJ, Brand MD. Topology of superoxide production from different sites in the mitochondrial electron transport chain. J. Biol. Chem. 2002; 277:44784–44790. [PubMed: 12237311]
3. Antonenkov VD, Grunau S, Ohlmeier S, Hiltunen JK. Peroxisomes are oxidative organelles. Antioxid. Redox. Signal. 2010; 13:525–537. [PubMed: 19958170]
4. O'Rourke B, Cortassa S, Aon MA. Mitochondrial ion channels: gatekeepers of life and death. Physiology (Bethesda). 2005; 20:303–315. [PubMed: 16174870]
5. Baines CP, Kaiser RA, Purcell NH, Blair NS, Osinska H, Hambleton MA, Brunskill EW, Sayen MR, Gottlieb RA, Dorn GW, Robbins J, Molkentin JD. Loss of cyclophilin D reveals a critical role for mitochondrial permeability transition in cell death. Nature. 2005; 434:658–662. [PubMed: 15800627]
6. Giorgio M, Trinei M, Migliaccio E, Pelicci PG. Hydrogen peroxide: a metabolic by-product or a common mediator of ageing signals? Nat. Rev. Mol. Cell Biol. 2007; 8:722–728. [PubMed: 17700625]
7. Sideris DP, Tokatlidis K. Oxidative protein folding in the mitochondrial intermembrane space. Antioxid. Redox. Signal. 2010; 13:1189–1204. [PubMed: 20214493]
8. Zweier JL, Talukder MA. The role of oxidants and free radicals in reperfusion injury. Cardiovasc. Res. 2006; 70:181–190. [PubMed: 16580655]
9. Matsuzaki S, Szweda LI, Humphries KM. Mitochondrial superoxide production and respiratory activity: biphasic response to ischemic duration. Arch. Biochem. Biophys. 2009; 484:87–93. [PubMed: 19467633]
10. Valko M, Leibfritz D, Moncol J, Cronin MT, Mazur M, Telser J. Free radicals and antioxidants in normal physiological functions and human disease. Int. J. Biochem. Cell Biol. 2007; 39:44–84. [PubMed: 16978905]
11. Efremov RG, Baradaran R, Sazanov LA. The architecture of respiratory complex I. Nature. 2010; 465:441–445. [PubMed: 20505720]
12. Ceconi C, Bernocchi P, Boraso A, Cargnoni A, Pepi P, Curello S, Ferrari R. New insights on myocardial pyridine nucleotides and thiol redox state in ischemia and reperfusion damage. Cardiovasc. Res. 2000; 47:586–594. [PubMed: 10963731]
13. Correa F, Garcia N, Robles C, Martinez-Abundis E, Zazueta C. Relationship between oxidative stress and mitochondrial function in the post-conditioned heart. J. Bioenerg. Biomembr. 2008; 40:599–606. [PubMed: 18989763]
14. Ceconi C, Cargnoni A, Francolini G, Parinello G, Ferrari R. Heart rate reduction with ivabradine improves energy metabolism and mechanical function of isolated ischaemic rabbit heart. Cardiovasc. Res. 2009; 84:72–82. [PubMed: 19477966]
15. Hill BG, Awe SO, Vladykovskaya E, Ahmed Y, Liu SQ, Bhatnagar A, Srivastava S. Myocardial ischaemia inhibits mitochondrial metabolism of 4-hydroxy-trans-2-nonenal. Biochem. J. 2009; 417:513–524. [PubMed: 18800966]
16. Ido Y. Pyridine nucleotide redox abnormalities in diabetes. Antioxid. Redox. Signal. 2007; 9:931–942. [PubMed: 17508915]
17. Wright RM, McManaman JL, Repine JE. Alcohol-induced breast cancer: a proposed mechanism. Free Radic. Biol. Med. 1999; 26:348–354. [PubMed: 9895226]
18. Drechsel DA, Patel M. Respiration-dependent H2O2 removal in brain mitochondria via the thioredoxin/peroxiredoxin system. J. Biol. Chem. 2010; 285:27850–27858. [PubMed: 20558743]
19. Sedlak E, Fabian M, Robinson NC, Musatov A. Ferricytochrome c protects mitochondrial cytochrome c oxidase against hydrogen peroxide-induced oxidative damage. Free Radic. Biol. Med. 2010 In press.
20. Forman HJ, Azzi A. On the virtual existence of superoxide anions in mitochondria: thoughts regarding its role in pathophysiology. FASEB J. 1997; 11:374–375. [PubMed: 9141504]

21. Semak I, Naumova M, Korik E, Terekhovich V, Wortsman J, Slominski A. A novel metabolic pathway of melatonin: oxidation by cytochrome C. Biochemistry. 2005; 44:9300–9307. [PubMed: 15981996]
22. Pereverzev MO, Vygodina TV, Konstantinov AA, Skulachev VP. Cytochrome c, an ideal antioxidant. Biochem. Soc. Trans. 2003; 31:1312–1315. [PubMed: 14641051]
23. Korshunov SS, Krasnikov BF, Pereverzev MO, Skulachev VP. The antioxidant functions of cytochrome c. FEBS Lett. 1999; 462:192–198. [PubMed: 10580118]
24. Kagan VE, Borisenko GG, Tyurina YY, Tyurin VA, Jiang J, Potapovich AI, Kini V, Amoscato AA, Fujii Y. Oxidative lipidomics of apoptosis: redox catalytic interactions of cytochrome c with cardiolipin and phosphatidylserine. Free Radic. Biol. Med. 2004; 37:1963–1985. [PubMed: 15544916]
25. Kagan VE, Bayir HA, Belikova NA, Kapralov O, Tyurina YY, Tyurin VA, Jiang J, Stoyanovsky DA, Wipf P, Kochanek PM, Greenberger JS, Pitt B, Shvedova AA, Borisenko G. Cytochrome c/cardiolipin relations in mitochondria: a kiss of death. Free Radic. Biol. Med. 2009; 46:1439–1453. [PubMed: 19285551]
26. Chen YR, Deterding LJ, Sturgeon BE, Tomer KB, Mason RP. Protein oxidation of cytochrome C by reactive halogen species enhances its peroxidase activity. J. Biol. Chem. 2002; 277:29781–29791. [PubMed: 12050149]
27. Abriata LA, Cassina A, Tortora V, Marin M, Souza JM, Castro L, Vila AJ, Radi R. Nitration of solvent-exposed tyrosine 74 on cytochrome c triggers heme ironmethionine 80 bond disruption. Nuclear magnetic resonance and optical spectroscopy studies. J. Biol. Chem. 2009; 284:17–26. [PubMed: 18974097]
28. Yang J, Liu X, Bhalla K, Kim CN, Ibrado AM, Cai J, Peng TI, Jones DP, Wang X. Prevention of apoptosis by Bcl-2: release of cytochrome c from mitochondria blocked. Science. 1997; 275:1129–1132. [PubMed: 9027314]
29. Kluck RM, Bossy-Wetzel E, Green DR, Newmeyer DD. The release of cytochrome c from mitochondria: a primary site for Bcl-2 regulation of apoptosis. Science. 1997; 275:1132–1136. [PubMed: 9027315]
30. De Biase PM, Paggi DA, Doctorovich F, Hildebrandt P, Estrin DA, Murgida DH, Marti MA. Molecular basis for the electric field modulation of cytochrome C structure and function. J. Am. Chem. Soc. 2009; 131:16248–16256. [PubMed: 19886701]
31. Everse J, Coates PW. Neurodegeneration and peroxidases. Neurobiol. Aging. 2009; 30:1011–1025. [PubMed: 18053617]
32. Liu KJ, Gast P, Moussavi M, Norby SW, Vahidi N, Walczak T, Wu M, Swartz HM. Lithium phthalocyanine: a probe for electron paramagnetic resonance oximetry in viable biological systems. Proc Natl Acad Sci U S A. 1993; 90:5438–5442. [PubMed: 8390665]
33. Zweier JL. Measurement of superoxide-derived free radicals in the reperfused heart. Evidence for a free radical mechanism of reperfusion injury. J. Biol. Chem. 1988; 263:1353–1357. [PubMed: 2826476]
34. Velayutham M, Villamena FA, Fishbein JC, Zweier JL. Cancer chemopreventive oltipraz generates superoxide anion radical. Arch Biochem Biophys. 2005; 435:83–88. [PubMed: 15680910]
35. Pullar JM, Vissers MC, Winterbourn CC. Glutathione oxidation by hypochlorous acid in endothelial cells produces glutathione sulfonamide as a major product but not glutathione disulfide. J Biol Chem. 2001; 276:22120–22125. [PubMed: 11283008]
36. Lawrence A, Jones CM, Wardman P, Burkitt MJ. Evidence for the role of a peroxidase compound I-type intermediate in the oxidation of glutathione, NADH, ascorbate, and dichlorofluorescin by cytochrome c/H2O2. Implications for oxidative stress during apoptosis. J. Biol. Chem. 2003; 278:29410–29419. [PubMed: 12748170]
37. Karoui H, Rockenbauer A, Pietri S, Tordo P. Spin trapping of superoxide in the presence of beta-cyclodextrins. Chem. Commun. (Camb). 2002:3030–3031. [PubMed: 12536801]
38. Vanderkooi JM, Erecinska M, Silver IA. Oxygen in mammalian tissue: methods of measurement and affinities of various reactions. Am J Physiol. 1991; 260:C1131–C1150. [PubMed: 2058649]

39. Simic MG, Taub IA, Tocci J, Hurwitz PA. Free radical reduction of ferricytochrome-C. Biochem. Biophys. Res. Commun. 1975; 62:161–167. [PubMed: 234221]
40. Velayutham M, Muthukumaran RB, Sostaric JZ, McCraken J, Fishbein JC, Zweier JL. Interactions of the major metabolite of the cancer chemopreventive drug oltipraz with cytochrome c: a novel pathway for cancer chemoprevention. Free Radic Biol. Med. 2007; 43:1076–1085. [PubMed: 17761303]
41. Forni LG, Willson RL. Thiyl and phenoxyl free radicals and NADH. Direct observation of one-electron oxidation. Biochem. J. 1986; 240:897–903. [PubMed: 3827879]
42. Buettner GR. On the reaction of superoxide with DMPO/.OOH. Free Radic Res Commun. 1990; 10:11–15. [PubMed: 2165980]
43. Belikova NA, Vladimirov YA, Osipov AN, Kapralov AA, Tyurin VA, Potapovich MV, Basova LV, Peterson J, Kurnikov IV, Kagan VE. Peroxidase activity and structural transitions of cytochrome c bound to cardiolipin-containing membranes. Biochemistry. 2006; 45:4998–5009. [PubMed: 16605268]
44. Orrenius S, Zhivotovsky B. Cardiolipin oxidation sets cytochrome c free. Nat Chem Biol. 2005; 1:188–189. [PubMed: 16408030]
45. Gonzalvez F, Gottlieb E. Cardiolipin: setting the beat of apoptosis. Apoptosis. 2007; 12:877–885. [PubMed: 17294083]
46. Vladimirov YA, Proskurnina EV, Izmailov DY, Novikov AA, Brusnichkin AV, Osipov AN, Kagan VE. Cardiolipin activates cytochrome c peroxidase activity since it facilitates H(2)O(2) access to heme. Biochemistry (Mosc). 2006; 71:998–1005. [PubMed: 17009954]
47. Kagan VE, Tyurin VA, Jiang J, Tyurina YY, Ritov VB, Amoscato AA, Osipov AN, Belikova NA, Kapralov AA, Kini V, Vlasova II, Zhao Q, Zou M, Di P, Svistunenko DA, Kurnikov IV, Borisenko GG. Cytochrome c acts as a cardiolipin oxygenase required for release of proapoptotic factors. Nat Chem Biol. 2005; 1:223–232. [PubMed: 16408039]
48. Tischler ME, Friedrichs D, Coll K, Williamson JR. Pyridine nucleotide distributions and enzyme mass action ratios in hepatocytes from fed and starved rats. Arch Biochem Biophys. 1977; 184:222–236. [PubMed: 21628]
49. Rutter J, Reick M, Wu LC, McKnight SL. Regulation of clock and NPAS2 DNA binding by the redox state of NAD cofactors. Science. 2001; 293:510–514. [PubMed: 11441146]
50. Williamson JR, Corkey BE. Assay of citric acid cycle intermediates and related compounds--update with tissue metabolite levels and intracellular distribution. Methods Enzymol. 1979; 55:200–222. [PubMed: 459841]
51. Cadenas E, Davies KJ. Mitochondrial free radical generation, oxidative stress, and aging. Free Radic Biol Med. 2000; 29:222–230. [PubMed: 11035250]
52. Antunes F, Cadenas E. Cellular titration of apoptosis with steady state concentrations of H(2)O(2): submicromolar levels of H(2)O(2) induce apoptosis through Fenton chemistry independent of the cellular thiol state. Free Radic Biol Med. 2001; 30:1008–1018. [PubMed: 11316581]
53. Kulagina NV, Michael AC. Monitoring hydrogen peroxide in the extracellular space of the brain with amperometric microsensors. Anal Chem. 2003; 75:4875–4881. [PubMed: 14674466]
54. Houstis N, Rosen ED, Lander ES. Reactive oxygen species have a causal role in multiple forms of insulin resistance. Nature. 2006; 440:944–948. [PubMed: 16612386]
55. Niethammer P, Grabher C, Look AT, Mitchison TJ. A tissue-scale gradient of hydrogen peroxide mediates rapid wound detection in zebrafish. Nature. 2009; 459:996–999. [PubMed: 19494811]
56. Vandeplassche G, Hermans C, Thone F, Borgers M. Stunned myocardium has increased mitochondrial NADH oxidase and ATPase activities. Cardioscience. 1991; 2:47–53. [PubMed: 1832316]
57. Vandeplassche G, Hermans C, Thone F, Borgers M. Mitochondrial hydrogen peroxide generation by NADH-oxidase activity following regional myocardial ischemia in the dog. J. Mol. Cell Cardiol. 1989; 21:383–392. [PubMed: 2746659]
58. Brahimi-Horn MC, Pouyssegur J. Oxygen, a source of life and stress. FEBS Lett. 2007; 581:3582–3591. [PubMed: 17586500]

59. Zhao X, He G, Chen YR, Pandian RP, Kuppusamy P, Zweier JL. Endothelium-derived nitric oxide regulates postischemic myocardial oxygenation and oxygen consumption by modulation of mitochondrial electron transport. Circulation. 2005; 111:2966–2972. [PubMed: 15939832]
60. Wang P, Zweier JL. Measurement of nitric oxide and peroxynitrite generation in the postischemic heart. Evidence for peroxynitrite-mediated reperfusion injury. J. Biol. Chem. 1996; 271:29223–29230. [PubMed: 8910581]
61. Godoy LC, Munoz-Pinedo C, Castro L, Cardaci S, Schonhoff CM, King M, Tortora V, Marin M, Miao Q, Jiang JF, Kapralov A, Jemmerson R, Silkstone GG, Patel JN, Evans JE, Wilson MT, Green DR, Kagan VE, Radi R, Mannick JB. Disruption of the M80-Fe ligation stimulates the translocation of cytochrome c to the cytoplasm and nucleus in nonapoptotic cells. Proc. Natl. Acad. Sci. USA. 2009; 106:2653–2658. [PubMed: 19196960]
62. Castro L, Eiserich JP, Sweeney S, Radi R, Freeman BA. Cytochrome c: a catalyst and target of nitrite-hydrogen peroxide-dependent protein nitration. Arch. Biochem. Biophys. 2004; 421:99–107. [PubMed: 14678790]
63. Schonheit K, Nohl H. Oxidation of cytosolic NADH via complex I of heart mitochondria. Arch. Biochem. Biophys. 1996; 327:319–323. [PubMed: 8619621]
64. Laraspata D, Gorgoglione V, La Piana G, Palmitessa V, Marzulli D, Lofrumento NE. Interaction of nitric oxide with the activity of cytosolic NADH/cytochrome c electron transport system. Arch. Biochem. Biophys. 2009; 489:99–109. [PubMed: 19653993]
65. La Piana G, Marzulli D, Consalvo MI, Lofrumento NE. Cytochrome c-induced cytosolic nicotinamide adenine dinucleotide oxidation, mitochondrial permeability transition, and apoptosis. Arch. Biochem. Biophys. 2003; 410:201–211. [PubMed: 12573279]
66. Batandier C, Leverve X, Fontaine E. Opening of the mitochondrial permeability transition pore induces reactive oxygen species production at the level of the respiratory chain complex I. J. Biol. Chem. 2004; 279:17197–17204. [PubMed: 14963044]
67. Petrosillo G, Moro N, Ruggiero FM, Paradies G. Melatonin inhibits cardiolipin peroxidation in mitochondria and prevents the mitochondrial permeability transition and cytochrome c release. Free Radic. Biol. Med. 2009; 47:969–974. [PubMed: 19577639]
68. Zorov DB, Juhaszova M, Sollott SJ. Mitochondrial ROS-induced ROS release: an update and review. Biochim. Biophys. Acta. 2006; 1757:509–517. [PubMed: 16829228]
69. Aon MA, Cortassa S, O'Rourke B. Mitochondrial oscillations in physiology and pathophysiology. Adv. Exp. Med. Biol. 2008; 641:98–117. [PubMed: 18783175]
70. Kurz FT, Aon MA, O'Rourke B, Armoundas AA. Spatio-temporal oscillations of individual mitochondria in cardiac myocytes reveal modulation of synchronized mitochondrial clusters. Proc. Natl. Acad. Sci. USA. 2010 In press.
71. Zorov DB, Filburn CR, Klotz LO, Zweier JL, Sollott SJ. Reactive oxygen species (ROS)-induced ROS release: a new phenomenon accompanying induction of the mitochondrial permeability transition in cardiac myocytes. J. Exp. Med. 2000; 192:1001–1014. [PubMed: 11015441]
72. Dispersyn GD, Borgers M. Apoptosis in the heart: about programmed cell death and survival. News Physiol. Sci. 2001; 16:41–47. [PubMed: 11390947]
73. Cheng Y, Zhu P, Yang J, Liu X, Dong S, Wang X, Chun B, Zhuang J, Zhang C. Ischaemic preconditioning-regulated miR-21 protects heart against ischaemia/reperfusion injury via anti-apoptosis through its target PDCD4. Cardiovasc. Res. 2010 In press.
74. Nur EKA, Gross SR, Pan Z, Balklava Z, Ma J, Liu LF. Nuclear translocation of cytochrome c during apoptosis. J. Biol. Chem. 2004; 279:24911–24914. [PubMed: 15073175]
75. Poot M, Pierce RH. Detection of changes in mitochondrial function during apoptosis by simultaneous staining with multiple fluorescent dyes and correlated multiparameter flow cytometry. Cytometry. 1999; 35:311–317. [PubMed: 10213196]
76. Zamzami N, Marchetti P, Castedo M, Decaudin D, Macho A, Hirsch T, Susin SA, Petit PX, Mignotte B, Kroemer G. Sequential reduction of mitochondrial transmembrane potential and generation of reactive oxygen species in early programmed cell death. J. Exp. Med. 1995; 182:367–377. [PubMed: 7629499]
77. Winterbourn CC. Reconciling the chemistry and biology of reactive oxygen species. Nat Chem Biol. 2008; 4:278–286. [PubMed: 18421291]

78. Cai J, Jones DP. Superoxide in apoptosis. Mitochondrial generation triggered by cytochrome c loss. J Biol Chem. 1998; 273:11401–11404. [PubMed: 9565547]
79. Zhao Y, Wang ZB, Xu JX. Effect of cytochrome c on the generation and elimination of O2*- and H2O2 in mitochondria. J Biol Chem. 2003; 278:2356–2360. [PubMed: 12435729]
80. Cassina AM, Hodara R, Souza JM, Thomson L, Castro L, Ischiropoulos H, Freeman BA, Radi R. Cytochrome c nitration by peroxynitrite. J. Biol. Chem. 2000; 275:21409–21415. [PubMed: 10770952]
81. Sivitz WI, Yorek MA. Mitochondrial dysfunction in diabetes: from molecular mechanisms to functional significance and therapeutic opportunities. Antioxid. Redox. Signal. 2010; 12:537–577. [PubMed: 19650713]
82. Addabbo F, Montagnani M, Goligorsky MS. Mitochondria and reactive oxygen species. Hypertension. 2009; 53:885–892. [PubMed: 19398655]
83. Kim YK, Lee MS, Son SM, Kim IJ, Lee WS, Rhim BY, Hong KW, Kim CD. Vascular NADH oxidase is involved in impaired endothelium-dependent vasodilation in OLETF rats, a model of type 2 diabetes. Diabetes. 2002; 51:522–527. [PubMed: 11812764]
84. Rajagopalan S, Kurz S, Munzel T, Tarpey M, Freeman BA, Griendling KK, Harrison DG. Angiotensin II-mediated hypertension in the rat increases vascular superoxide production via membrane NADH/NADPH oxidase activation. Contribution to alterations of vasomotor tone. J. Clin. Invest. 1996; 97:1916–1923. [PubMed: 8621776]
85. Cardounel AJ, Cui H, Samouilov A, Johnson W, Kearns P, Tsai AL, Berka V, Zweier JL. Evidence for the pathophysiological role of endogenous methylarginines in regulation of endothelial NO production and vascular function. J. Biol. Chem. 2007; 282:879–887. [PubMed: 17082183]
86. Bian K, Murad F. Nitric oxide (NO)--biogeneration, regulation, and relevance to human diseases. Front. Biosci. 2003; 8:d264–d278. [PubMed: 12456375]
87. Witting PK, Rayner BS, Wu BJ, Ellis NA, Stocker R. Hydrogen peroxide promotes endothelial dysfunction by stimulating multiple sources of superoxide anion radical production and decreasing nitric oxide bioavailability. Cell Physiol. Biochem. 2007; 20:255–268. [PubMed: 17762155]
88. Ellis EA, Guberski DL, Hutson B, Grant MB. Time course of NADH oxidase, inducible nitric oxide synthase and peroxynitrite in diabetic retinopathy in the BBZ/WOR rat. Nitric Oxide. 2002; 6:295–304. [PubMed: 12009847]
89. Vaughn AE, Deshmukh M. Glucose metabolism inhibits apoptosis in neurons and cancer cells by redox inactivation of cytochrome c. Nat. Cell Biol. 2008; 10:1477–1483. [PubMed: 19029908]
90. Le Belle JE, Orozco NM, Paucar AA, Saxe JP, Mottahedeh J, Pyle AD, Wu H, Kornblum HI. Proliferative neural stem cells have high endogenous ROS levels that regulate self-renewal and neurogenesis in a PI3K/Akt-dependant manner. Cell Stem Cell. 8:59–71. [PubMed: 21211782]
91. Jang YY, Sharkis SJ. A low level of reactive oxygen species selects for primitive hematopoietic stem cells that may reside in the low-oxygenic niche. Blood. 2007; 110:3056–3063. [PubMed: 17595331]
92. Schriner SE, Ogburn CE, Smith AC, Newcomb TG, Ladiges WC, Dolle ME, Vijg J, Fukuchi K, Martin GM. Levels of DNA damage are unaltered in mice overexpressing human catalase in nuclei. Free Radic. Biol. Med. 2000; 29:664–673. [PubMed: 11033419]
93. Zhao Y, Wang ZB, Xu JX. Effect of cytochrome c on the generation and elimination of O2*- and H2O2 in mitochondria. J. Biol. Chem. 2003; 278:2356–2360. [PubMed: 12435729]
94. Liu Z, Lin H, Ye S, Liu QY, Meng Z, Zhang CM, Xia Y, Margoliash E, Rao Z, Liu XJ. Remarkably high activities of testicular cytochrome c in destroying reactive oxygen species and in triggering apoptosis. Proc Natl Acad Sci U S A. 2006; 103:8965–8970. [PubMed: 16757556]
95. Zhao Y, Xu JX. The operation of the alternative electron-leak pathways mediated by cytochrome c in mitochondria. Biochem Biophys Res Commun. 2004; 317:980–987. [PubMed: 15094365]
96. Barros MH, Netto LE, Kowaltowski AJ. H(2)O(2) generation in Saccharomyces cerevisiae respiratory pet mutants: effect of cytochrome c. Free Radic Biol Med. 2003; 35:179–188. [PubMed: 12853074]
97. Martin H, Eckerskorn C, Gartner F, Rassow J, Lottspeich F, Pfanner N. The yeast mitochondrial intermembrane space: purification and analysis of two distinct fractions. Anal. Biochem. 1998; 265:123–128. [PubMed: 9866716]

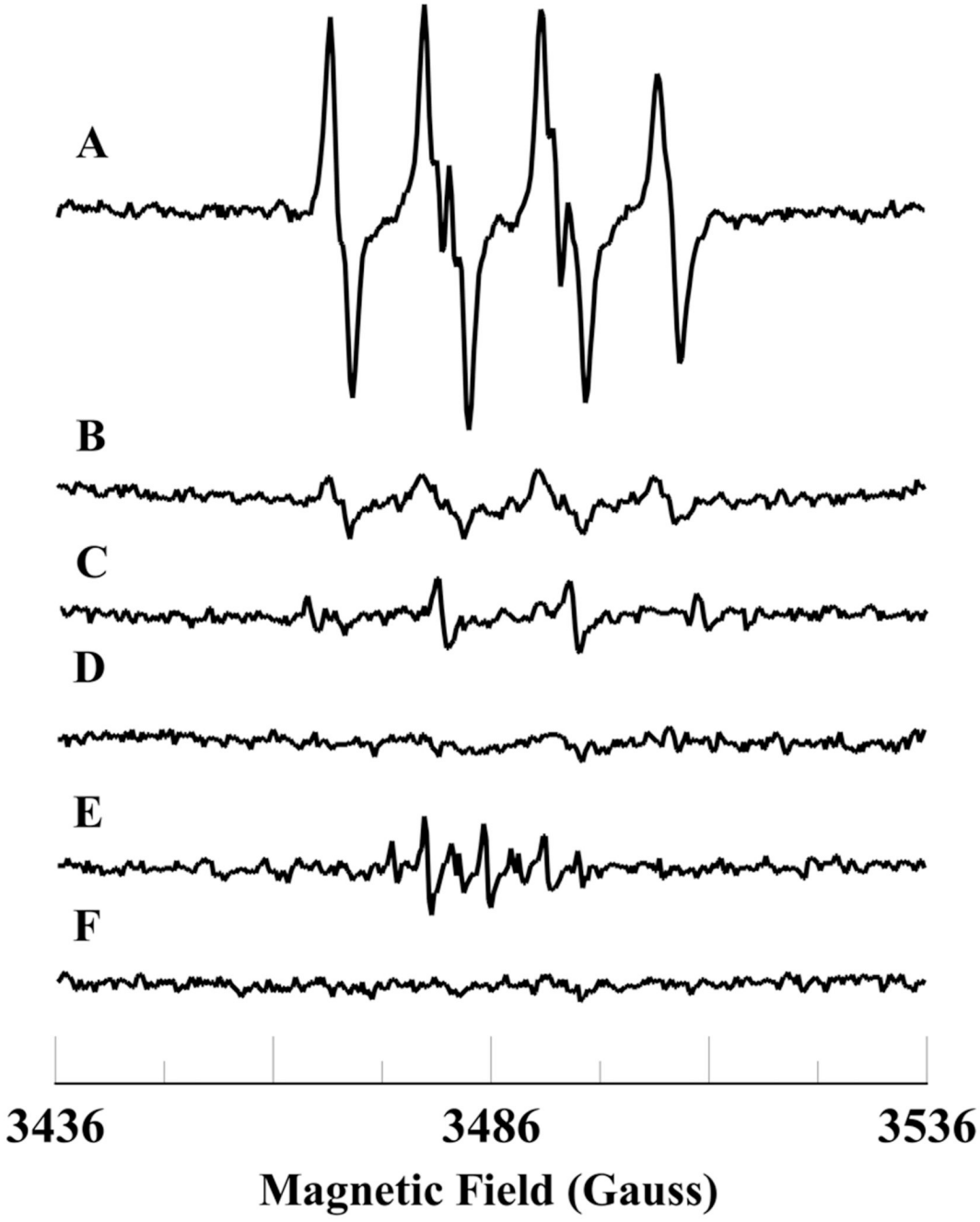

Figure 1.

Room temperature EPR spectra of the superoxide radical adduct of DMPO, DMPO-OOH. All the reactions were performed in 50 mM phosphate buffer (pH = 7.4) containing 0.1 mM DTPA. Spectrum A: DMPO (50 mM), methyl-β-cyclodextrin (0.1 M), Fe^{3+}cyt c (0.1 mM), NADH (1 mM), and H_2O_2 (0.5 mM). Spectrum B: DMPO (50 mM), methyl-β-cyclodextrin (0.1 M), NADH (1 mM), and H_2O_2 (0.5 mM). Spectrum C: DMPO (50 mM), Fe^{3+}cyt c (0.1 mM), NADH (1 mM), and H_2O_2 (0.5 mM). Spectrum D: DMPO (50 mM), methyl-β-cyclodextrin (0.1 M), Fe^{3+}cyt c (0.1 mM), SOD1 (500 U/mL), NADH (1 mM), and H_2O_2 (0.5 mM). Spectrum E: DMPO (50 mM), methyl-β-cyclodextrin (0.1 M), Fe^{3+}cyt c (0.1 mM), and H_2O_2 (0.5 mM). Spectrum F: DMPO (50 mM), methyl-β-cyclodextrin (0.1 M),

Fe^{3+}cyt c (0.1 mM), and NADH (1 mM). The observed isotropic hyperfine values of the DMPO-OOH adducts are a_N = 13.49 G, a_{H1} = 10.78 G, and a_{H2} = 1.39 G. EPR instrument parameters used were as described in the materials and methods section.

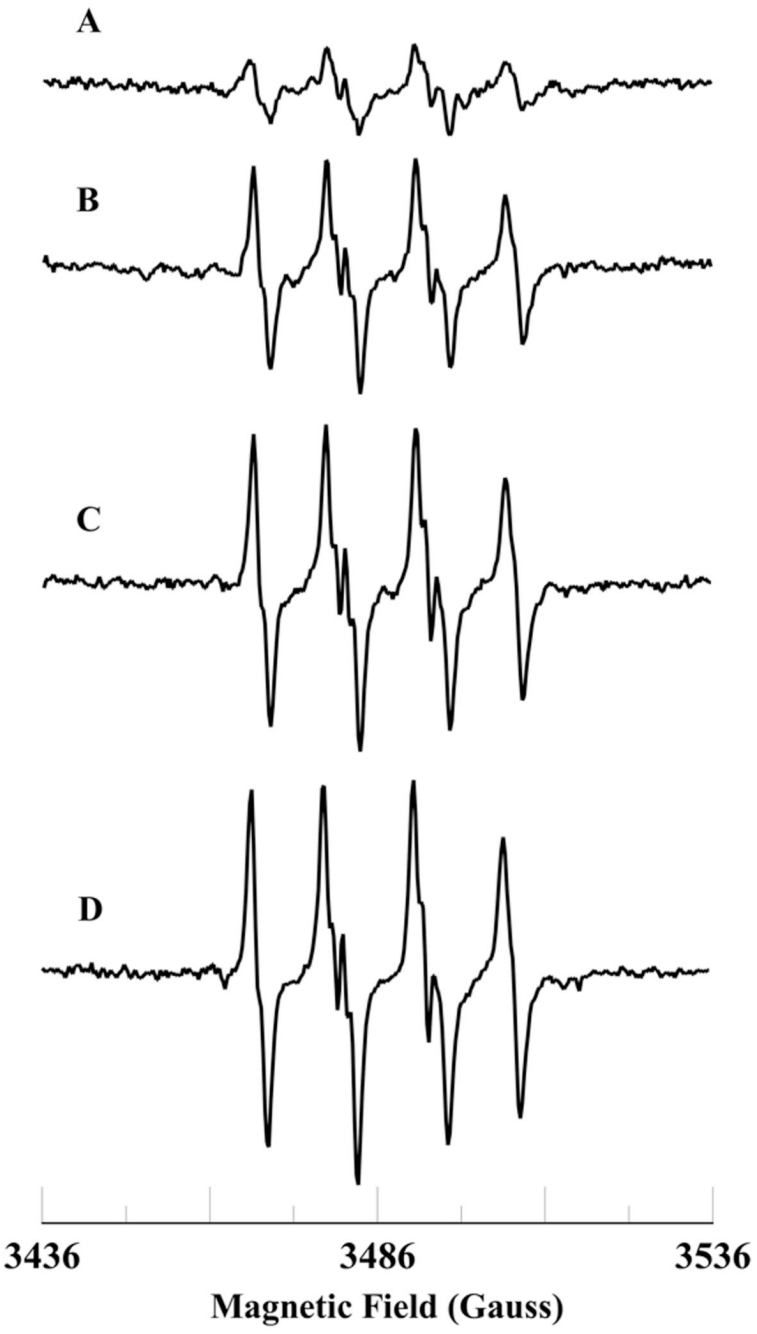

Figure 2.

Room temperature EPR spectra of the superoxide radical adduct of DMPO, DMPO-OOH. All the reactions were performed in 50 mM phosphate buffer (pH = 7.4) containing 0.1 mM DTPA. Spectrum A: DMPO (50 mM), methyl-β-cyclodextrin (0.1 M), Fe^{3+}cyt c (0.1 mM), NADH (0.1 mM), and H_2O_2 (0.5 mM). Spectrum B: DMPO (50 mM), methyl-β-cyclodextrin (0.1 M), Fe^{3+}cyt c (0.1 mM), NADH (0.5 mM), and H_2O_2 (0.5 mM). Spectrum C: DMPO (50 mM), methyl-β-cyclodextrin (0.1 M), Fe^{3+}cyt c (0.1 mM), NADH (1 mM), and H_2O_2 (0.5 mM). Spectrum D: DMPO (50 mM), methyl-β-cyclodextrin (0.1 M), Fe^{3+}cyt c (0.1 mM), NADH (2 mM), and H_2O_2 (0.5 mM). EPR instrument parameters used were as described in the materials and methods section.

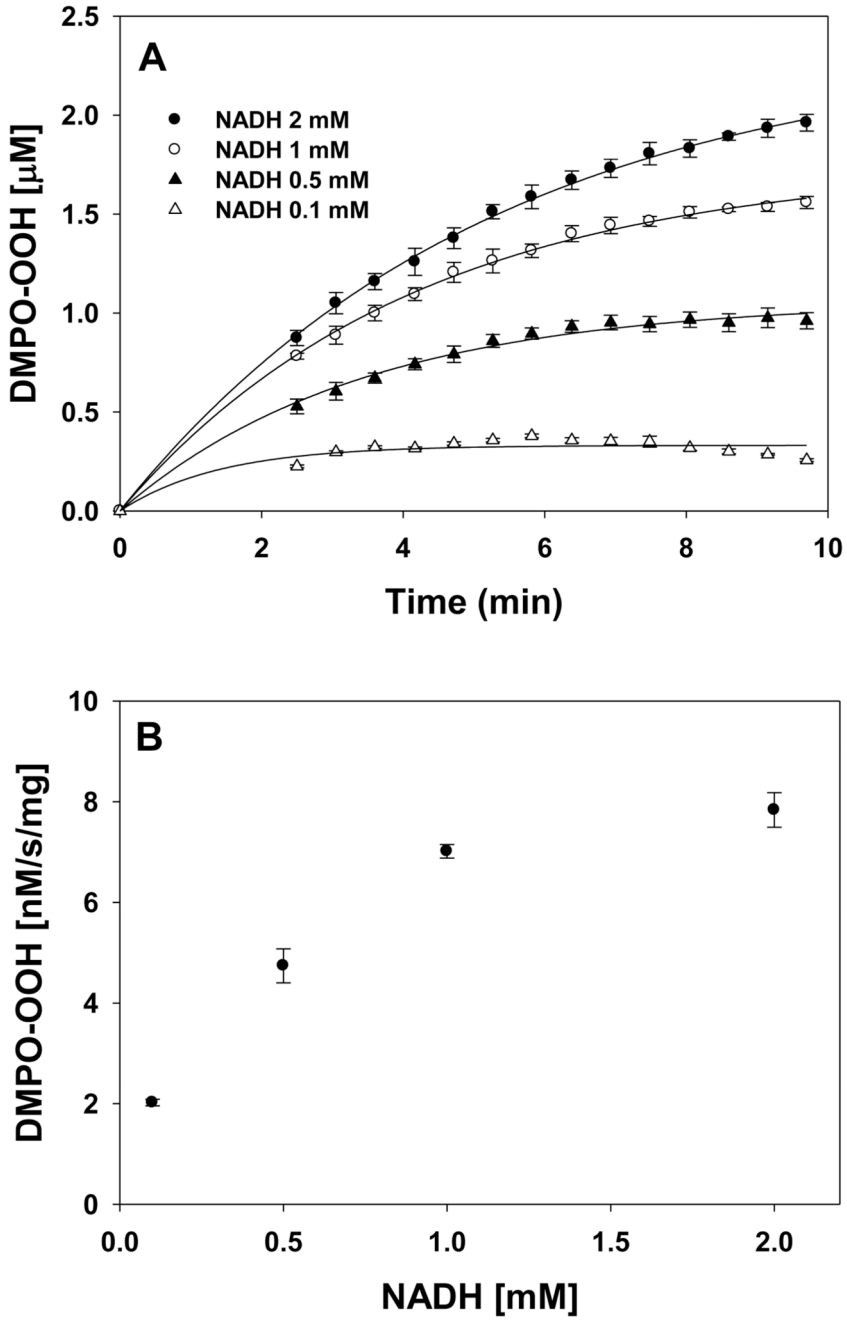

Figure 3.

(A) Plot of the concentration of superoxide radical adduct of DMPO (DMPO-OOH) vs time for various concentrations of NADH. Experiments were performed with DMPO (50 mM), methyl-β-cyclodextrin (0.1 M), Fe^{3+}cyt c (0.1 mM), H_2O_2 (0.5 mM) and various concentrations of NADH in phosphate buffer containing DTPA (0.1 mM). (B) Plot of initial rate of formation of superoxide radical adducts of DMPO (DMPO-OOH) vs NADH concentrations. Rates in panel B were obtained from the initial slope of the data from panel A. EPR spectra were quantified by computer simulation of the spectra and comparison of the double integral of the observed signal with that of a TEMPO standard (1 μM) measured under the identical conditions. Data represent means ± S.E (n = 3).

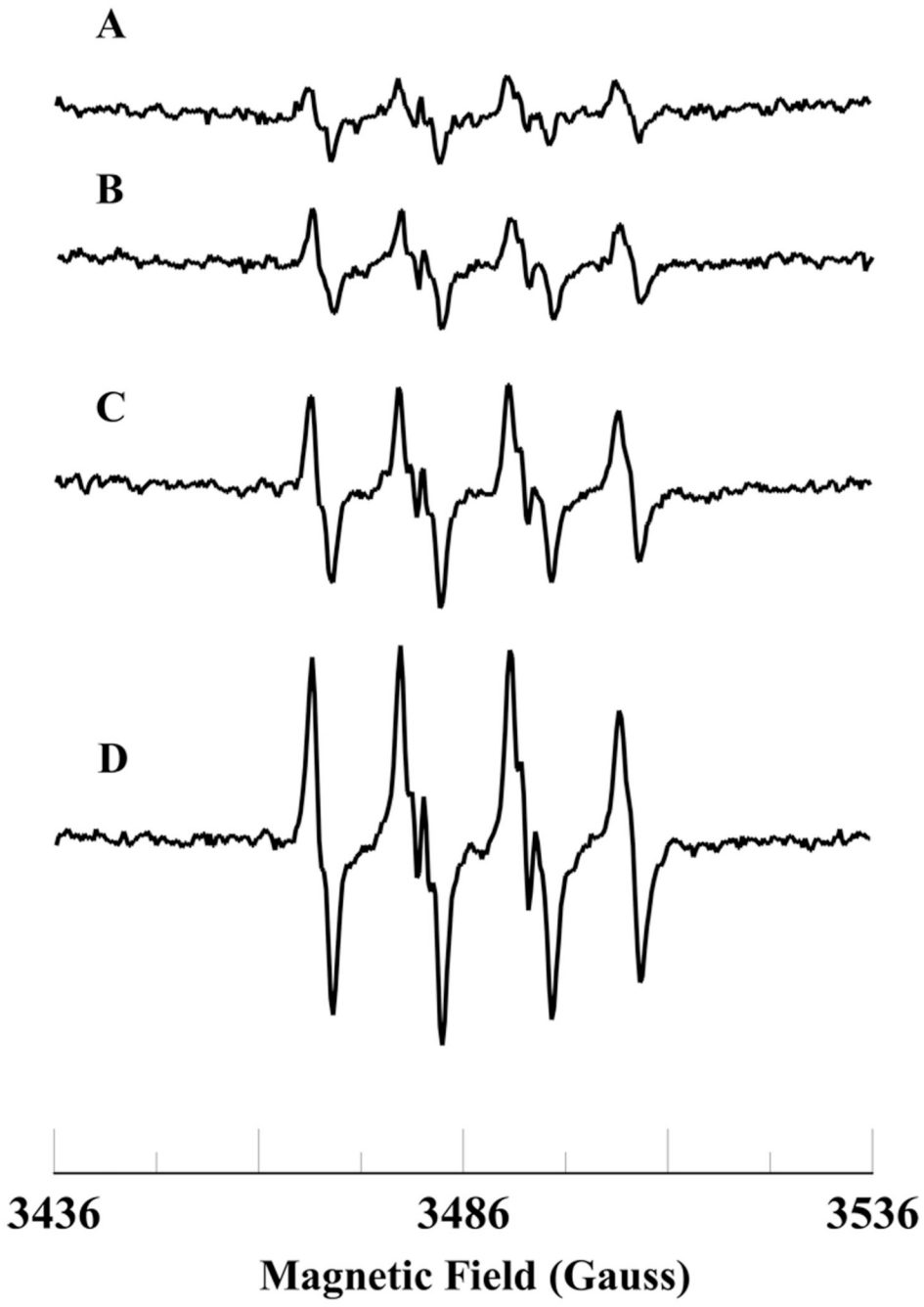

Figure 4.

Room temperature EPR spectra of the superoxide radical adduct of DMPO, DMPO-OOH. All the reactions were performed in 50 mM phosphate buffer (pH = 7.4) containing 0.1 mM DTPA. Spectrum A: DMPO (50 mM), methyl-β-cyclodextrin (0.1 M), Fe^{3+}cyt c (0.1 mM), NADH (1 mM), and H_2O_2 (0.05 mM). Spectrum B: DMPO (50 mM), methyl-β-cyclodextrin (0.1 M), Fe^{3+}cyt c (0.1 mM), NADH (1 mM), and H_2O_2 (0.1 mM). Spectrum C: DMPO (50 mM), methyl-β-cyclodextrin (0.1 M), Fe^{3+}cyt c (0.1 mM), NADH (1 mM), and H_2O_2 (0.25 mM). Spectrum D: DMPO (50 mM), methyl-β-cyclodextrin (0.1 M), Fe^{3+}cyt c (0.1 mM), NADH (1 mM), and H_2O_2 (0.5 mM). EPR instrument parameters used were as described in the materials and methods section.

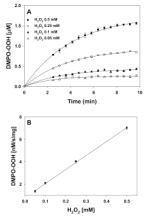

Figure 5.

(A) Plot of the concentration of superoxide radical adduct of DMPO (DMPO-OOH) vs time for various concentrations of H_2O_2. Experiments were performed with DMPO (50 mM), methyl-β-cyclodextrin (0.1 M), Fe^{3+}cyt c (0.1 mM), NADH (1 mM), and various concentrations of H_2O_2 in phosphate buffer containing DTPA (0.1 mM). (B) Plot of initial rate of formation of superoxide radical adducts of DMPO (DMPO-OOH) vs H_2O_2 concentrations. Rates in panel B were obtained from the initial slope of the data from panel A. EPR spectra were quantified by computer simulation of the spectra and comparison of the double integral of the observed signal with that of a TEMPO standard (1 μM) measured under the identical conditions. Data represent means ± S.E (n = 3).

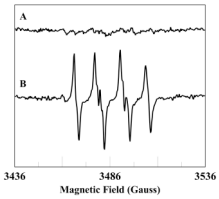

Figure 6.

Room temperature EPR spectra of the superoxide radical adduct of DMPO, DMPO-OOH. All the reactions were performed in 50 mM phosphate buffer (pH = 7.4) containing 0.1 mM DTPA. The reaction mixture contains DMPO (50 mM), methyl-β-cyclodextrin (0.1 M), Fe^{3+}cyt c (0.1 mM), NADH (1 mM), and H_2O_2 (0.5 mM). Spectrum A: The reaction mixture was prepared inside the nitrogen filled glove box. Spectrum B: The reactants were taken out from the glove box and the reaction mixture was prepared under room air. EPR instrument parameters used were as described in the materials and methods section.

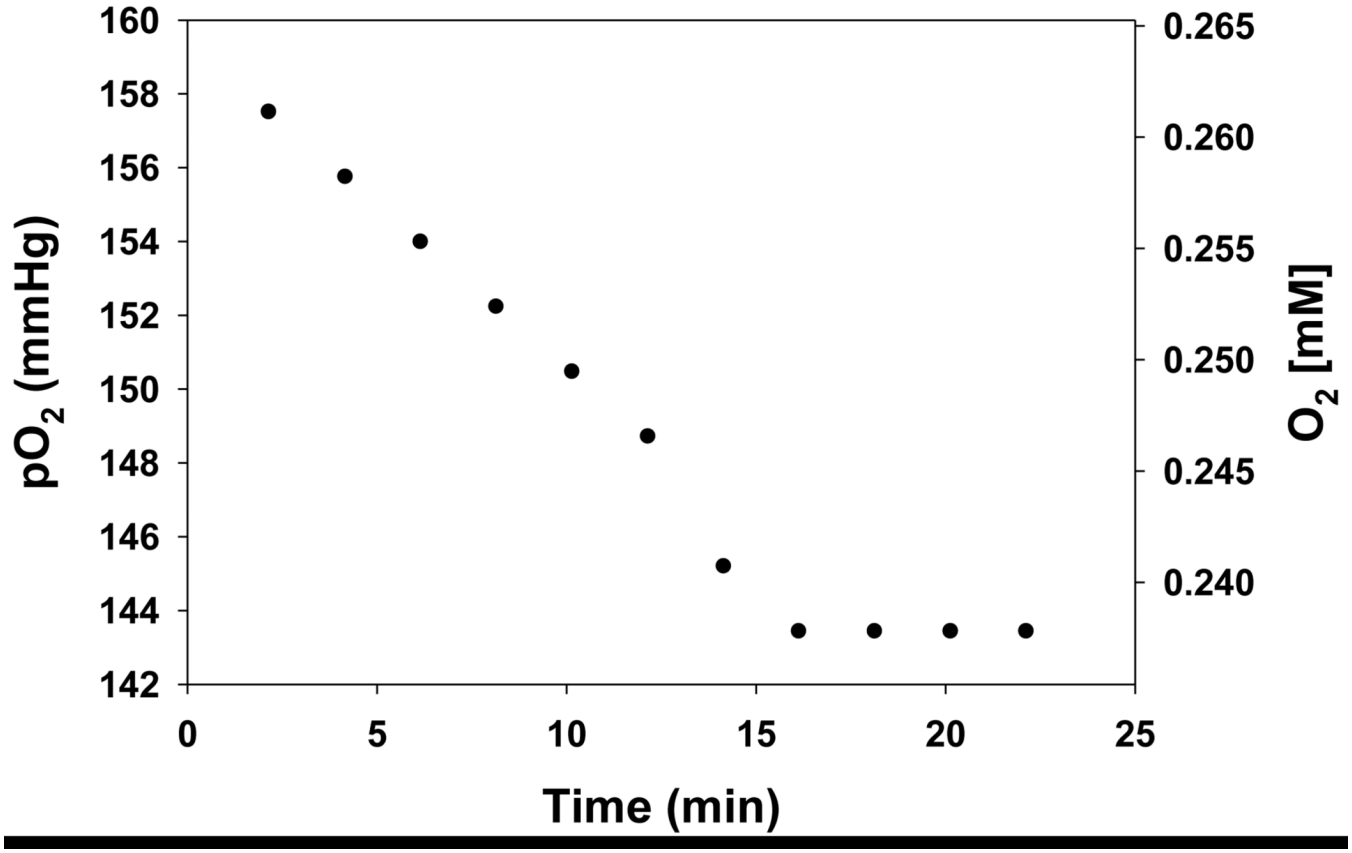

Figure 7.

Plot of the oxygen consumption in phosphate buffer containing Fe^{3+}cyt c (0.1 mM), NADH (1 mM), and H_2O_2 (0.5 mM) using the EPR oximetry probe LiPc. Line width from the EPR spectra were converted into partial pressure of oxygen using the calibration formula of pO_2 = (Line width G − 0.1748)/0.005684. EPR instrument parameters used were microwave frequency 9.775, modulation frequency 100 kHz, modulation amplitude 0.1 G, microwave power 1 mW, number of scans 1, scan time 10.5 s, and time constant 82 ms. The partial pressure of oxygen was converted into dissolved concentration based on the solubility of oxygen in water at room air of 0.265 mM [38].

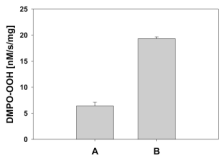

Figure 8.

Oxidation of Fe^{3+}cyt c to M-Fe^{3+}cyt c by HOCl increases the initial rate of formation of superoxide radical adducts of DMPO (DMPO-OOH). The preparation of M-Fe^{3+}cyt c is described in the materials and methods section. EPR spin trapping experiments were performed with DMPO (50 mM), methyl-β-cyclodextrin (0.1 M), Fe^{3+}cyt c/M-Fe^{3+}cyt c (0.1 mM), NADH (1 mM), and H_2O_2 (0.5 mM) in phosphate buffer containing DTPA (0.1 mM). A: Fe^{3+}cyt c. B: M-Fe^{3+}cyt c. EPR spectra were quantified by computer simulation of the spectra and comparison of the double integral of the observed signal with that of a TEMPO standard (1 μM) measured under the identical conditions. Initial rates were calculated and mean ± S.E shown in graph (n = 3).

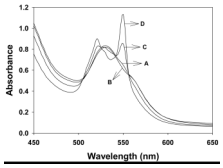

Figure 9.

UV-visible absorption spectra of cyt c in phosphate buffer, pH 7.4. Experiments were performed with Fe^{3+}cyt c, NADH, and H_2O_2. Reactions were initiated by the addition of H_2O_2. Spectra were recorded five minutes after mixing all the reactants. A: Fe^{3+}cyt c (0.1 mM), B: Fe^{3+}cyt c (0.1 mM) and H_2O_2 (0.5 mM), C: Fe^{3+}cyt c (0.1 mM) and NADH (2 mM), D: Fe^{3+}cyt c (0.1 mM), NADH (2 mM), and H_2O_2 (0.5 mM).

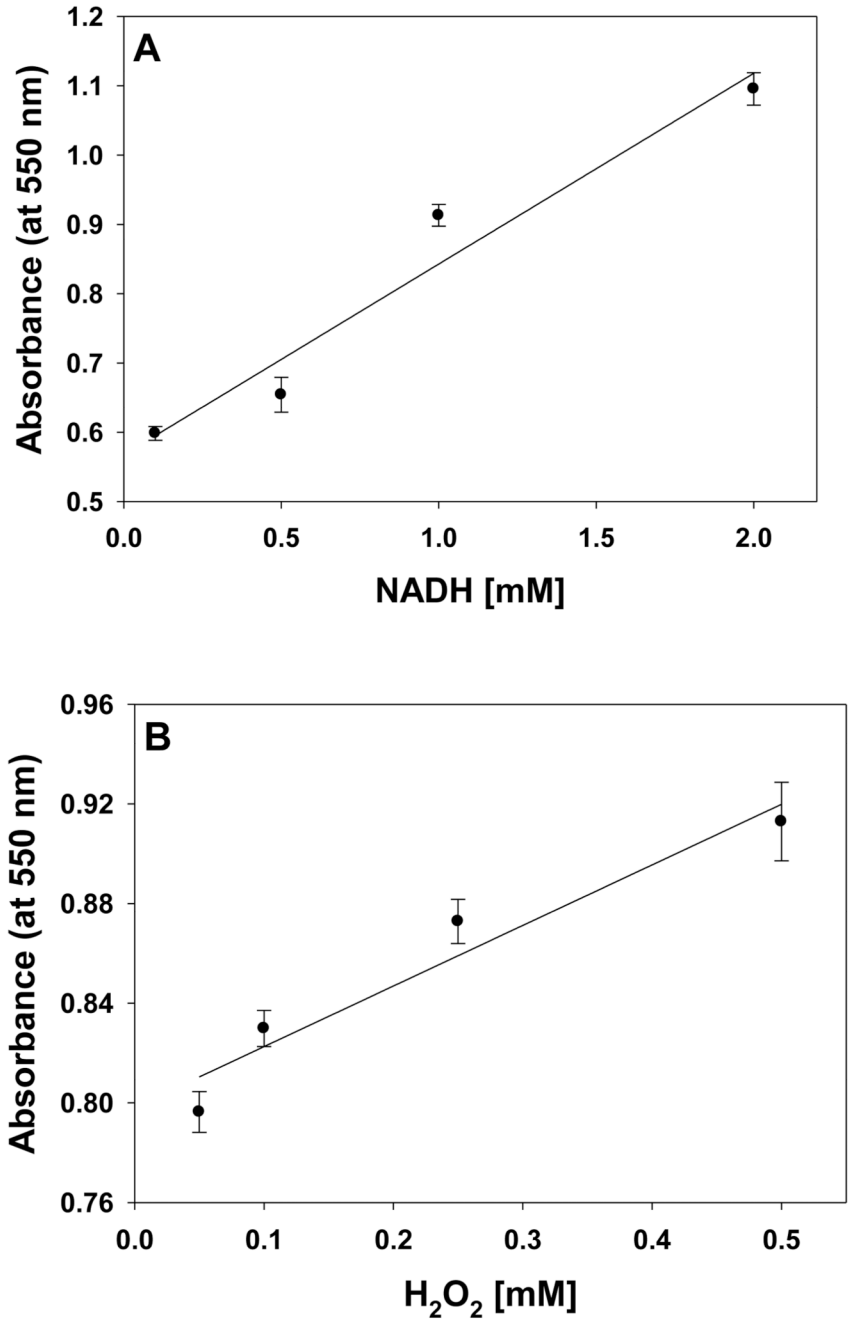

Figure 10.

The effect of NADH and H_2O_2 on the reduction of Fe^{3+}cyt c in phosphate buffer, pH 7.4. Experiments were performed with Fe^{3+}cyt c, NADH, and H_2O_2. Reactions were initiated by the addition of H_2O_2. UV-visible absorption spectra were recorded five minutes after mixing all the reactants. A: Fe^{3+}cyt c (0.1 mM), NADH (0.1 – 2 mM), and H_2O_2 (0.5 mM). B: Fe^{3+}cyt c (0.1 mM), NADH (1 mM), and H_2O_2 (0.05 – 0.5 mM). Data represent means ± S.E (n = 3).

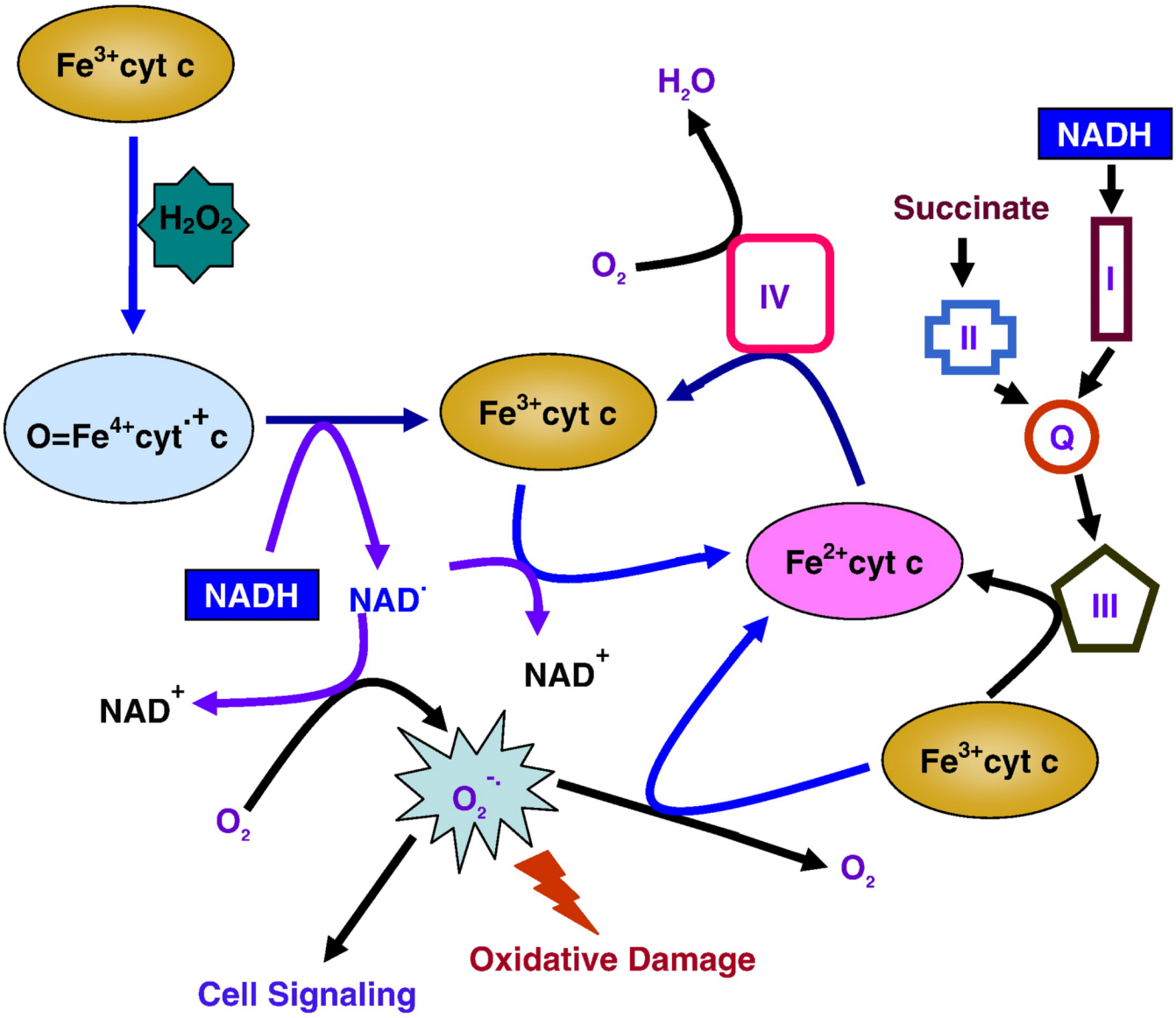

Figure 11.
Proposed model of cytochrome c mediated removal of H_2O_2, oxidation of NADH, generation of superoxide radical, and alternative electron transfer pathway in mitochondria.

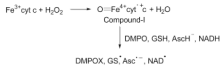

Scheme 1.

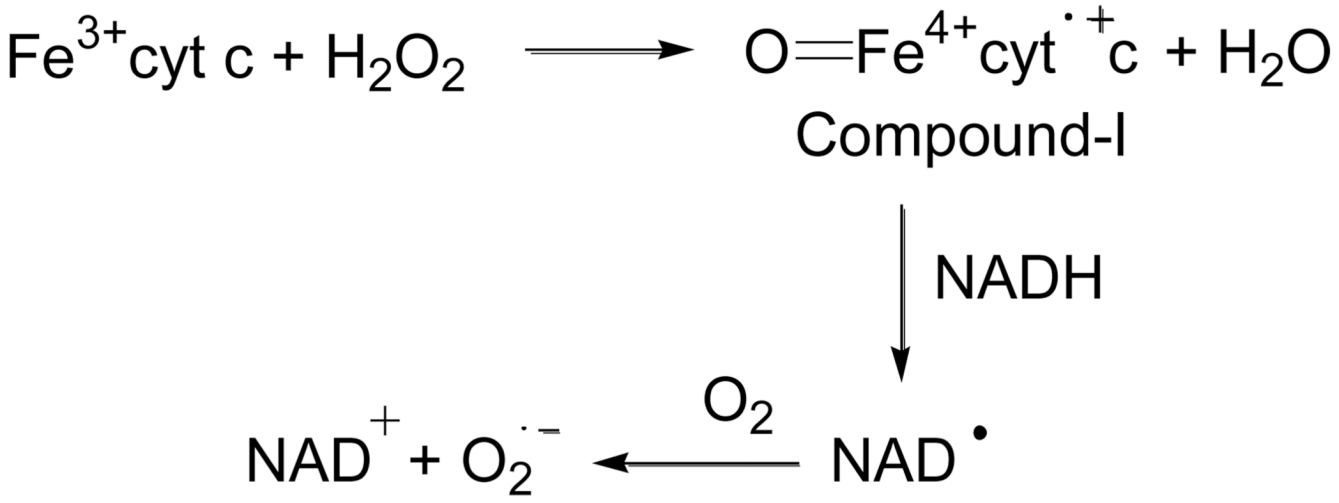

Scheme 2.